International Symposium
On Turbulence and Shear Flow
Phenomena (TSFP-8)
August 28 - 30, 2013 Poitiers, France

ON THE FUNDAMENTAL FLUCTUATING WALL-SHEAR-STRESS

Olivier Cabrit
Department of Mechanical Engineering
University of Melbourne
Victoria 3010, Australia
o.cabrit@unimelb.edu.au

Romain Mathis
Laboratoire de Mécanique de Lille
CNRS UMR 8107, Université Lille Nord de France
59655 Villeneuve dAscq, France
romain.mathis@univ-lille1.fr

Ivan Marusic
Department of Mechanical Engineering
University of Melbourne
Victoria 3010, Australia
imarusic@unimelb.edu.au

ABSTRACT

Recent studies by Marusic *et al.* (2010) and Mathis *et al.* (2013) suggest the existence of a fundamental wall-shear-stress in any wall-bounded turbulent flow. It can be interpreted as a background turbulent wall-shear-stress free of Reynolds number effects. To investigate its universal aspect, here we report a statistical/spectral comparison of this fundamental wall-shear-stress in three different configurations: boundary layer, pipe, and channel flows. A model is proposed to generate a synthetic fundamental fluctuating wall-shear-stress surface, which can then be used to predict the 2D wall-shear-stress at any Reynolds number thanks to an inner-outer scale interaction model.

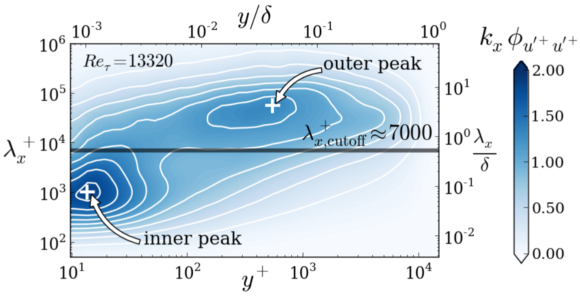

Figure 1. Streamwise premultiplied energy spectrogram of streamwise velocity fluctuation in a turbulent boundary layer. Measurements by Kulandaivelu (2012).

INTRODUCTION

In the past decade, the increase of the Reynolds number in numerical simulations and experiments of turbulent wall-bounded flows has considerably improved the knowledge and understanding of the fluctuating velocity field. It is now well accepted (Hutchins and Marusic, 2007a) that two main energetic ranges of scales exist within such wall-bounded flows. Indeed, as depicted in Figure 1, two distinct peaks are identified in the streamwise premultiplied energy spectrogram: an inner peak occurring near the wall, around $y^+ \approx 15$, and an outer peak appearing in the logarithmic region ($y^+_{\mathrm{ml}} \approx \sqrt{15 Re_\tau}$) which becomes more prominent as the Reynolds number increases (Hutchins and Marusic, 2007a; Kim and Adrian, 1999; Tomkins and Adrian, 2003; amongst others).

Note the notations used in this paper: y denotes the wall-normal direction, u the streamwise velocity, Re_τ the friction Reynolds number based on the boundary layer thickness δ and the friction velocity $u_\tau = \sqrt{\overline{\tau}/\rho}$, $\overline{\tau}$ is the mean streamwise component of the wall-shear-stress (the spanwise component is not considered in this paper), prime denotes a fluctuating quantity (*i.e.* whose mean value was substracted), and "+" superscript a quantity scaled in wall units.

Many authors have considered the possible coupling between the prominent scales, and their interaction appears to be well described by a superposition mechanism (Hutchins and Marusic, 2007a; Abe *et al.*, 2004), and an amplitude modulation effect (Hutchins and Marusic, 2007b; Bandyopadhyay and Hussain, 1984; Mathis *et al.*, 2009). Following these observations, Marusic *et al.* (2010) and Mathis *et al.* (2011) proposed a conceptual approach embedding the superposition/modulation mechanisms into an inner-outer scale interaction (IOSI) model. Given the large scale part of the fluctuating velocity field at the middle of the logarithmic layer, this model is notably able to predict the high-order statistics and the spectral content of the fluctuating velocity in the vicinity of the wall ($0 \le y^+ \le 100$, say). Recently, Mathis *et al.* (2013) extended the model to the fluctuating component of the streamwise wall-shear-stress, τ'. It is formulated as follows:

$$\tau'^+ = \tau'^* \left[1 + \alpha\, \widetilde{u'^+_{\theta_L}}\right] + \alpha\, \widetilde{u'^+_{\theta_L}}, \qquad (1)$$

where $\widetilde{u'^+_{\theta_L}}$ is the large scale fluctuating velocity taken at the middle of the log-layer (cutoff wavelength set to $\lambda^+_{x,\mathrm{cutoff}} = 7000$) and shifted in the streamwise direction in order to respect the large-scale structure angle θ_L (Mathis *et al.*, 2013), α is the superposition/modulation coefficient, and τ'^* the so-called fundamental fluctuating wall-shear-stress, which can be interpreted as an inner-scaled shear-stress neither affected by the superposition effect, nor by the amplitude modulation effect. In their paper, Mathis *et al.* (2013) made use of the direct numerical simulation of channel flow by del Álamo *et al.* (2004) ($Re_\tau = 934$) in order to extract τ'^*, and demonstrated the efficacy of the IOSI model over a wide range of Reynolds numbers.

In the following, we analyse direct numerical simulations of boundary layer, channel, and pipe flows in order to verify the universal aspect of the fundamental wall-shear-stress and to investigate its statistical properties and 1D/2D spectral content. We also present a model to generate a synthetic surface of fundamental wall-shear-stress fluctuations respecting both the fundamental probability density function (PDF) and its 1D/2D energy spectra.

BOUNDARY LAYER, PIPE AND CHANNEL FLOWS

The difference between boundary layer, pipe and channel flows is investigated thanks to a numerical database whose Reynolds number remains relatively constant: Schlatter *et al.* (2009) for boundary layer ($Re_\tau = 1250$), Chin *et al.* (2010) for pipe ($Re_\tau = 1000$), and del Álamo *et al.* (2004) for channel ($Re_\tau = 934$) flows.
For the three configurations, the fundamental wall-shear-stress, τ'^*, is first extracted using the procedure proposed by Mathis *et al.* (2013), *i.e.* the cutoff wavelength separating the inner and outer peaks is set to $\lambda^+_{x,\text{cutoff}} = 7000$ and taken at the middle of the log-layer, $y^+ \approx \sqrt{15Re_\tau}$. Note also that the superposition/modulation coefficient has been set to $\alpha = 0.1$ in all cases, as found by Mathis *et al.* (2013). The first results shown in Figures 2 and 3 support the universal aspect of τ'^* regarding both its probability density function and streamwise 1D energy spectrum. To further highlight the similarities between the three flows, the standard deviation, skewness, and kurtosis are also presented in Table 1. Interestingly, the probability density function has the features previously reported in the literature at low Reynolds numbers (Alfredsson *et al.*, 1988; Örlü and Schlatter, 2011), which supports the idea that τ'^* can be seen as a fundamental turbulent wall-shear-stress, free of the large scale effects appearing at high Reynolds numbers.

Table 1. Standard deviation, skewness and kurtosis of the fundamental wall-shear-stress.

Configuration	τ'^*_{rms}	$Sk(\tau'^*)$	$Ku(\tau'^*)$
Boundary Layer	0.41	1.02	5.1
Channel	0.40	1.07	5.1
Pipe	0.40	0.99	5.0
pdf model, eq. (2)	0.40	1.01	4.77
1D spectra model, eq. (3)	0.40	n/a	n/a
2D spectra model, eq. (4)	0.40	n/a	n/a

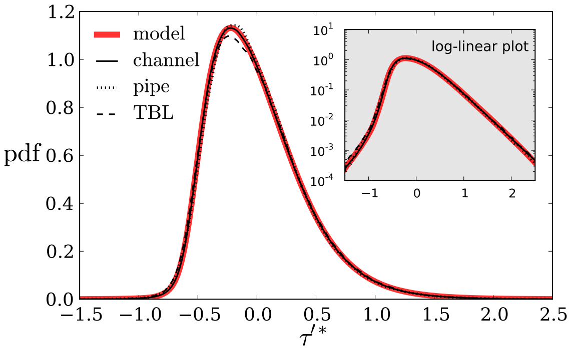

Figure 2. Probability density function of the fundamental wall-shear-stress in channel ($Re_\tau = 934$), pipe ($Re_\tau = 1000$), and boundary layer ($Re_\tau = 1250$) flows compared to the model equation (2).

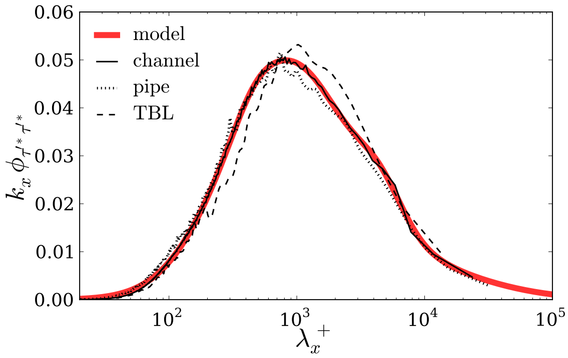

Figure 3. Streamwise premultiplied 1D energy spectrum of the fundamental wall-shear-stress in channel ($Re_\tau = 934$), pipe ($Re_\tau = 1000$), and boundary layer ($Re_\tau = 1250$) flows compared to the model equation (3).

Based on these strong similarities, we postulate the idea of manufacturing two model functions for both the probability density function and the premultiplied energy spectrum. Due to their respective shape (which reaches zero at the extremities and stays positive in the middle), we propose to model these functions using a least-squares optimisation of the coefficients of multiple superposed Gaussian-type functions as formulated in equations (2) and (3). We respectively need nine and four superposed Gaussian-functions to reach a good level of accuracy (relative integral error below 1%) and notably capture the tails of the PDF as depicted in Figure 2. The final optimised parameters retained are summarised in Tables 2 and 3, and the corresponding three first order moments are reported in Table 1. It must be noted at this stage that the integration of the energy spectrum model Eq. (3) gives the same variance as the one contained in the probability density function Eq. (2) with a three-digits round-off precision. This is a cornerstone of the model proposed here since this is the only common property shared by both the probability density function and energy spectrum.

$$\text{pdf}(\tau'^*) = \sum_{i=1}^{9} A_i\, e^{\frac{-(\tau'^*-a_i)^2}{2\alpha_i^2}} \tag{2}$$

$$k_x\phi_{\tau'^*\tau'^*} = \sum_{i=1}^{4} B_i\, e^{\frac{-\ln^2 \frac{\lambda_x^+}{b_i}}{2\beta_i^2}} \tag{3}$$

Table 2. Coefficients of the PDF model equation (2).

i	A_i	a_i	α_i
1	4.434×10^{-1}	-0.157	0.187
2	4.391×10^{-1}	-0.331	0.143
3	3.471×10^{-1}	0.045	0.249
4	2.660×10^{-1}	0.201	0.361
5	2.184×10^{-1}	-0.463	0.110
6	7.254×10^{-2}	0.437	0.490
7	1.548×10^{-2}	0.568	0.709
8	3.871×10^{-3}	-0.766	0.066
9	1.749×10^{-8}	-0.507	1.679

Table 3. Coefficients of the premultiplied energy spectrum model equation (3).

i	B_i	b_i	β_i
1	4.613×10^{-2}	811	1.104
2	7.527×10^{-3}	5452	1.477
3	6.668×10^{-3}	4543	0.408
4	2.250×10^{-3}	452	0.341

A SYNTHETIC FUNDAMENTAL WALL-SHEAR-STRESS

Thanks to these two model functions, Eq. (2) and Eq. (3), we can make use of an Iterative Amplitude Adjusted Fourier Transform (IAAFT) algorithm (Schreiber and Schmitz, 2000) in order to generate a synthetic fundamental wall-shear-stress that respects both the required spectral content and the probability density function. The algorithm is composed of the following steps:

❶ generate a random series satisfying the PDF Eq. (2);
❷ compute the Fourier transform of this series;
❸ replace the amplitude of the Fourier coefficients with the ones satisfying the energy spectra Eq. (3) (the phase being unchanged);
❹ compute the inverse Fourier transform;
❺ replace the maximum value of the new signal ④ by the maximum value of the random series initially generated at step ①, do the same for the second maximum value, and so on until the minimum value is replaced;
❻ repeat steps ② to ⑤ until convergence.

Note that after step ④, the target energy spectra is perfectly satisfied whereas the PDF is not converged. The opposite happens after step ⑥ where the target PDF is perfectly satisfied. Hence, the actual quantity converging during the iterative procedure is the spectral density, and its convergence is obviously better satisfied if the model functions, Eq. (2) and Eq. (3), share the same variance, which is the case here. In practice, this algorithm converges quickly, 15 iterations being generally sufficient to generate a synthetic 1D signal of fundamental wall-shear-stress.

To assess the quality and usefulness of this surrogate signal, we propose to inject it into the IOSI model Eq. (1) and to verify that it does not deteriorate the model predictions obtained with a fundamental signal originally extracted from the channel flow DNS (results noted "original" hereafter). Figure 4 depicts the wall-shear-stress standard deviation predicted over the range of Reynolds numbers experimentally studied by Kulandaivelu (2012). The predictions involving the synthetic signal match the original predictions with a very good level of accuracy, and the Reynolds number trend observed by Schlatter & Örlü (2010) is preserved. We also present in Figure 5 the PDF and 1D premultiplied energy spectrum predicted thanks to an input large scale streamwise velocity taken from a turbulent boundary layer experiment at $Re_\tau = 13320$. Even if the reference data does not exist because of the difficulty to measure velocity fluctuations very close to the wall with hot-wire anemometry (Hutchins *et al.*, 2009), we can still notice that the prediction involving the synthetic signal stays in fairly good agreement. This level of agreement is also found for the other Reynolds numbers investigated ($2740 \leq Re_\tau \leq 22884$, not shown here), which supports the quality of the synthetic fundamental wall-shear-stress.

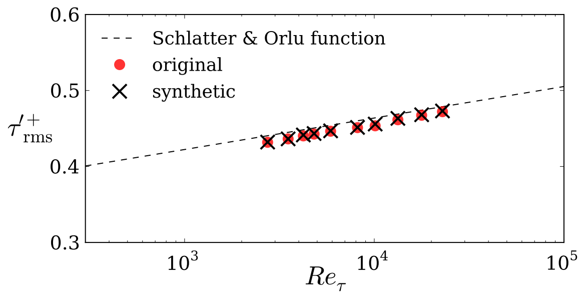

Figure 4. Standard deviation of the wall-shear-stress predicted by Eq. (1) with the original fundamental signal and the synthetic one. The Schlatter & Örlü (2010) function is also plotted as a reference.

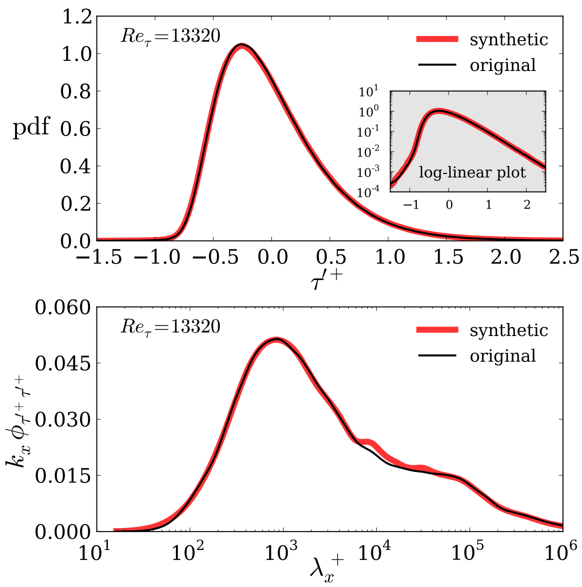

Figure 5. PDF (top) and 1D premultiplied energy spectrum (bottom) predicted by the IOSI model Eq. (1). Input large scale velocity taken from a turbulent boundary layer experiment at $Re_\tau = 13320$ by Kulandaivelu (2012).

2D FUNDAMENTAL WALL-SHEAR-STRESS

So far, the model functions, Eq. (2) and Eq. (3), coupled with the IAAFT algorithm allow us to generate a synthetic fundamental signal. Because this signal is one-dimensional, it can be useful for hot-wire measurements. However, if one wants to use the IOSI model Eq. (1) with a numerical simulation (a large-eddy simulation for instance), it is necessary to extend the study to the spanwise direction. We recall that the spanwise component is not considered in this study.

To this end, we present in Figure 6 the spanwise spectrogram of the streamwise fluctuating velocity in a turbulent boundary layer simulation by Schlatter *et al.* (2009) at $Re_\tau = 1250$. Altough the Reynolds number is moderate, it is high enough to observe the emergence of the outer peak (this peak is not fully formed in the channel flow at $Re_\tau = 934$). This is an interesting result as an outer peak cannot be observed on the streamwise spectrogram for such a Reynolds number (the outer peak tends to emerge around $Re_\tau \approx 5000$ on the streamwise spectrogram). As for the streamwise spectrogram, the inner peak is located at $y^+ \approx 15$, and its characteristic spanwise wavelength is $\lambda_z^+ \approx 120$ which corresponds to the near-wall streaks spanwise spacing. The outer peak is located in the middle of the logarithmic region $y^+_{\text{ml}} \approx \sqrt{15 Re_\tau}$, as is also the case with the streamwise spectrogram.

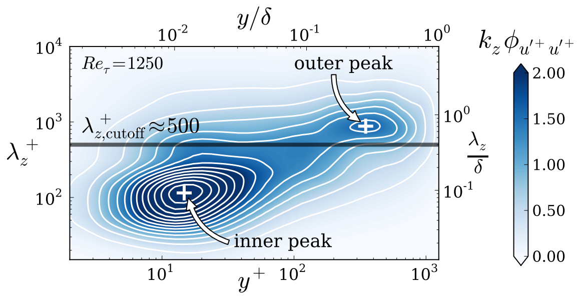

Figure 6. Spanwise premultiplied energy spectrogram of the streamwise velocity fluctuation in a turbulent boundary layer. Simulation by Schlatter *et al.* (2009).

This observation allows us to extend the concept of the IOSI model developed by Marusic *et al.* (2010) and Mathis *et al.* (2011) in the spanwise direction. The main concept of the IOSI model is to isolate the Reynolds number effects (related to the outer peak) from the fundamental small scale turbulence (associated with the near-wall cycle and the inner peak). For the streamwise direction, the cutoff wavelength was set to $\lambda^+_{x,\text{cutoff}} = 7000$ by Mathis *et al.* (2011). Here, the spanwise spectrogram suggests a spanwise cutoff wavelength of $\lambda^+_{z,\text{cutoff}} = 500$ to isolate the two peaks.

Hence, we can consider again the channel simulation by del Álamo *et al.* (2004) and use these characteristic cutoff wavelengths to spectrally filter (sharp cutoff filter) the simulation. This 2D filtering gives access to the large scale streamwise velocity fluctuation, $\widetilde{u'^+_{\theta_L}}$, which can be used to extract the 2D fundamental wall-shear-stress by inverting Eq. (1). Note that the value of α and θ_L are unchanged to do so because the spanwise filtering should not change the structure angle nor the superposition/modulation coefficient if the spanwise cutoff only filters the inner peak. In addition, we use only the channel simulation at this stage as it is the one for which we have the most instantaneous fields available. Indeed, with 15 instantaneous fields and making use of both the top and bottom walls of the channel, one can extract 30 independent fundamental wall-shear-stress planes. It ensures a good convergence of the probability density function and energy spectra.

As expected the 2D filtering procedure did not drastically change the probability density function compared to that obtained with the 1D procedure. The new PDF is not shown here but its first order moments (standard deviation, skewness and kurtosis) respect the ones of the model function, Eq. (2). This indicates that the spanwise cutoff has been well chosen to isolate the inner and outer peaks.

The 2D energy spectrum of the fundamental wall-shear-stress is shown in Figure 7. To propose a model function of this 2D energy spectrum, we now decide to optimise the parameters of multiple superposed 2D Gaussian-functions expressed as follows:

$$k_x k_z \phi_{\tau'^*\tau'^*} = \sum_{i=1}^{7} C_i\, e^{-\mathscr{A}\ln^2\frac{\lambda_x^+}{\Lambda_{x,i}} - \mathscr{B}\ln\frac{\lambda_x^+}{\Lambda_{x,i}}\ln\frac{\lambda_z^+}{\Lambda_{z,i}} - \mathscr{C}\ln^2\frac{\lambda_z^+}{\Lambda_{z,i}}}, \quad (4)$$

where,

$$\mathscr{A} = \frac{\cos^2\Theta_i}{2\gamma_{x,i}^2} + \frac{\sin^2\Theta_i}{2\gamma_{z,i}^2}, \quad (5)$$

$$\mathscr{B} = \frac{\sin 2\Theta_i}{2\gamma_{z,i}^2} - \frac{\sin 2\Theta_i}{2\gamma_{x,i}^2}, \quad (6)$$

$$\mathscr{C} = \frac{\sin^2\Theta_i}{2\gamma_{x,i}^2} + \frac{\cos^2\Theta_i}{2\gamma_{z,i}^2}. \quad (7)$$

The use of seven Gaussian-functions and a least-squares optimisation is sufficient to find the set of optimised parameters presented in Table 4. Hence, the model function proposed, Eq. (4-7), gives very good agreement as depicted in Figure 7. Furthermore, when the model function is integrated over the streamwise/spanwise wavelengths, it also preserves the desired standard deviation as shown in Table 1.

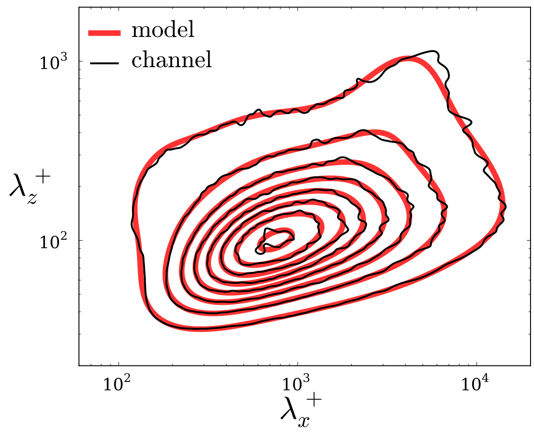

Figure 7. 2D premultiplied energy spectrum of the fundamental wall-shear-stress extracted from the channel flow simulation by del Álamo *et al.* (2004) at $Re_\tau = 934$. The model function, Eq. (4-7), is also plotted. Levels are from 4×10^{-3} to 3.2×10^{-2} every 4×10^{-3}.

Table 4. Coefficients of the 2D energy spectrum model function, Eq. (4-7).

i	C_i	$\Lambda_{x,i}$	$\Lambda_{z,i}$	$\gamma_{x,i}$	$\gamma_{z,i}$	Θ_i
1	1.750×10^{-2}	533	81	0.774	0.383	-29.796
2	1.491×10^{-2}	1332	107	1.117	0.500	-4.909
3	5.869×10^{-3}	1159	214	0.679	1.227	$+83.624$
4	2.687×10^{-3}	2597	337	1.449	0.443	-62.109
5	2.560×10^{-3}	7510	359	0.635	1.427	-37.558
6	1.848×10^{-3}	435	540	1.194	0.987	$+77.216$
7	1.828×10^{-3}	135	217	0.741	0.392	-66.827

2D WALL-SHEAR-STRESS PREDICTIONS

Finally, the IAAFT algorithm presented above is enriched by the use of the 2D energy spectrum model function, Eq. (4-7), instead of using the 1D energy spectrum model. This allows us to generate a synthetic plane of streamwise fluctuating fundamental wall-shear-stress which can then be used in the IOSI model, Eq. (1). Figure 8 shows a zoom of the instantaneous wall-shear-stress fluctuations taken in the DNS of del Álamo *et al.* (2004), compared to a prediction involving the fundamental wall-shear-stress extracted from the same DNS (but at a different time), and a prediction involving the 2D synthetic fundamental wall-shear-stress. The overall agreement is very good, notably for the high-shear macroscopic regions which are located at the same locations.

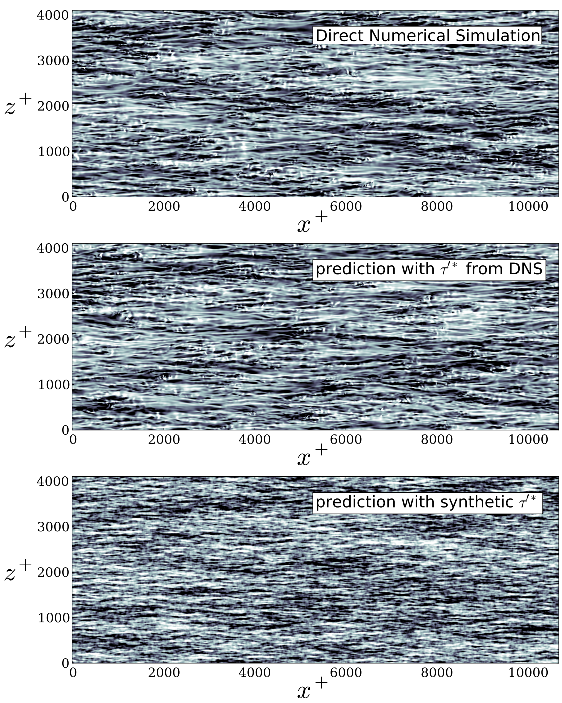

Figure 8. Instantaneous wall-shear-stress at $Re_\tau = 934$ for a channel flow. Black and white regions corresponds to high and low shear-stresses, respectively. Simulation by del Álamo *et al.* (2004) (top), IOSI prediction using a fundamental signal extracted from the DNS (middle), and IOSI prediction using a fundamental 2D synthetic surface (bottom).

It must be emphasised that even if the prediction involving the synthetic field appears accurate, it still seems that the wall-shear-stress is less organised giving a "blurry" aspect to the prediction. This is due to the fact that nothing is done to model the phase of the fundamental wall-shear-stress. Indeed, when the IAAFT algorithm is applied, at step ❸, the phase is simply preserved from the previous step. This means that the algorithm naturally reorganises the random phase initially imposed at step ❶, sufficiently to recover the first order moments, but not in a fashion able to reproduce an equivalent coherent aspect. However, as shown in Figure 9, this apparent lack of organisation is not visible on spatial streamwise/spanwise auto-correlations attesting the good level of fidelity of the prediction involving the synthetic model proposed in this paper.

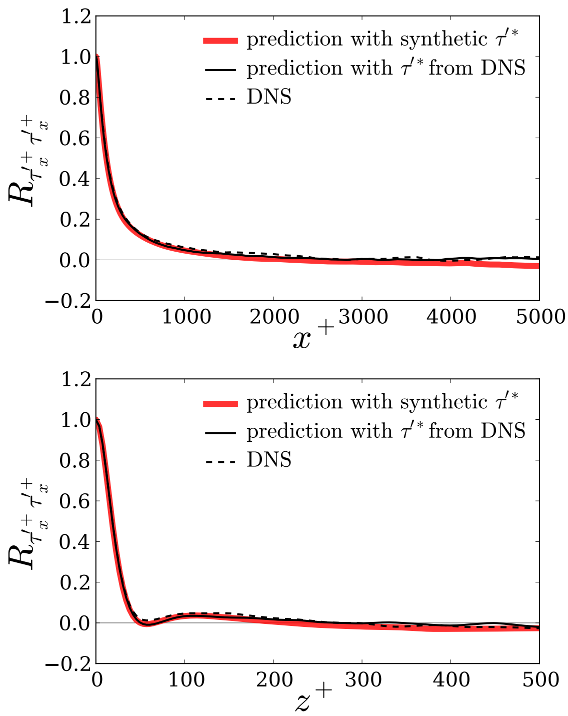

Figure 9. Normalised auto-correlations of the predicted fluctuating wall-shear-stress in streamwise direction (top) and spanwise direction (bottom).

CONCLUSION

This paper discusses the existence of the so-called fundamental wall-shear-stress, investigating a numerical database of turbulent boundary layer, pipe, and channel flows. The fundamental wall-shear-stress extracted from these three flows are found to be very close to each other, thus supporting the notion that a universal signal can be used. Based on these observations, model functions are formulated to represent its probability density function and its 1D/2D energy spectra. Coupled with an iterative amplitude adjusted Fourier transform algorithm, these model functions allow us to generate synthetic 1D signals, and 2D surfaces of fundamental wall-shear-stress.

The resulting synthetic signal can then be used with the inner-outer scale interaction model to predict instantaneous wall-shear-stress planes, where the only input is a 2D large scale streamwise velocity field taken in the middle of the logarithmic region. In this paper we make use of a filtered direct numerical simulation to provide this large scale field, but large-eddy simulations, or spanwise distributed hot-wire measurements could have also been used to reconstruct an instantaneous prediction of the wall-shear-stress at any Reynolds number.

While the predictions could be enhanced by taking into account the information contained in the fundamental wall-shear-stress phase, the procedure developed in this paper can still be used as a wall-model able to capture the Reynolds number dependency of both the high-order moments and spatial 2-point correlations of the wall-shear-stress.

ACKNOWLEDGEMENTS

The authors wish to acknowledge the support of the Australian Research Council and the University of Melbourne McKenzie Fellowship program.

REFERENCES

Abe, H., Kawamura, H. & Choi, H. 2004 Very large-scale structures and their effects on the wall shear-stress fluctuations in a turbulent channel flow up to $Re_\tau = 640$. *J. Fluids Eng.* **126** (5), 835–843.

del Álamo, J. C., Jiménez, J., Zandonade, P. & Moser, R. D. 2004 Scaling of the energy spectra of turbulent channels. *J. Fluid Mech.* **500**, 135–144.

Alfredsson, P. H., Johansson, A. V., Haritonidis, J. H. & Eckelmann, H. 1988 The fluctuating wall-shear stress and the velocity field in the viscous sublayer. *Phys. Fluids* **31** (5), 1026–1033.

Bandyopadhyay, P. R. & Hussain, A. K. M. F. 1984 The coupling between scales in shear flows. *Phys. Fluids* **27** (9), 2221–2228.

Chin, C., Ooi, A. S. H., Marusic, I. & Blackburn, H. M. 2010 The influence of pipe length on turbulence statistics computed from direct numerical simulation data. *Phys. Fluids* **22** (11), 115107.

Hutchins, N. & Marusic, I. 2007*a* Evidence of very long meandering features in the logarithmic region of turbulent boundary layers. *J. Fluid Mech.* **579**, 1–28.

Hutchins, N. & Marusic, I. 2007*b* Large-scale influences in near-wall turbulence. *Phil. Trans. R. Soc. A* **365**, 647–664.

Hutchins, N., Nickels, T. B., Marusic, I. & Chong, M. S. 2009 Hot-wire spatial resolution issues in wall-bounded turbulence. *J. Fluid Mech.* **635**, 103–136.

Kim, K. C. & Adrian, R. J. 1999 Very large-scale motion in the outer layer. *Phys. Fluids* **11** (2), 417–422.

Kulandaivelu, V. 2012 Evolution and structure of zero pressure gradient turbulent boundary layer. PhD thesis, The University of Melbourne, Melbourne, Victoria, Australia.

Marusic, I., Mathis, R. & Hutchins, N. 2010 Predictive model for wall-bounded turbulent flow. *Science* **239** (5988), 193–196.

Mathis, R., Hutchins, N. & Marusic, I. 2009 Large-scale amplitude modulation of the small-scale structures in turbulent boundary layers. *J. Fluid Mech.* **628**, 311–337.

Mathis, R., Hutchins, N. & Marusic, I. 2011 A predictive inner–outer model for streamwise turbulence statistics in wall-bounded flows. *J. Fluid Mech.* **681**, 537–566.

Mathis, R., Marusic, I., Chernyshenko, S. I. & Hutchins, N. 2013 Estimating wall-shear-stress fluctuations given an outer region input. *J. Fluid Mech.* **715**, 163–180.

Örlü, R. & Schlatter, P. 2011 On the fluctuating wall-shear stress in zero pressure-gradient turbulent boundary layer flows. *Phys. Fluids* **23** (2), 021704.

Schlatter, P. & Örlü, R. 2010 Assessment of direct numerical simulation data of turbulent boundary layers. *J. Fluid Mech.* **659**, 116–126.

Schlatter, P., Örlü, R., Li, Q., Brethouwer, G., Fransson, J. H. M., Johansson, A. V., Alfredsson, P. H. & Henningson, D. S. 2009 Turbulent boundary layers up to $Re_\theta = 2500$ studied through simulation and experiment. *Phys. Fluids* **21** (5), 051702.

Schreiber, T. & Schmitz, A. 2000 Surrogate time series. *Physica D* **142** (3-4), 346–382.

Tomkins, C. D. & Adrian, R. J. 2003 Spanwise structure and scale growth in turbulent boundary layers. *J. Fluid Mech.* **490**, 37–74.